USING X-RAY MICRO-COMPUTED TOMOGRAPHY TO EXAMINE VARIATIONS IN SHAPE OF BASALTIC AND QUARTZOFELDSPATHIC AEOLIAN AND FLUVIAL SEDIMENTS. K.G. Mason[1], R.C. Ewing[1], J. W. Bullard[1], S. A. Eckley[2], [1]Texas A&M University, College Station, TX 77843, [2]Jacobs Technology, NASA Johnson Space Center, Houston, TX 77058. (kgmason@tamu.edu)

Introduction: Sediments and sedimentary rocks contain a rich record of modern and ancient surface processes, climate, and environment [1]. The size and shape of the particles comprising the sediments and rocks are key to determining the provenance, transport history, and specific types of environments [2]. Such interpretations, however, depend on our ability to accurately characterize and disentangle the effects of source material, alteration, and energies in environments on particle size and shape. Here, we explore the use of 3D analysis from micro x-ray computed tomography (µXCT) data in assessing the environmental history of particles of different mineralogies (quartzofeldspathic and basaltic) and shaped by different process (aeolian and fluvial).

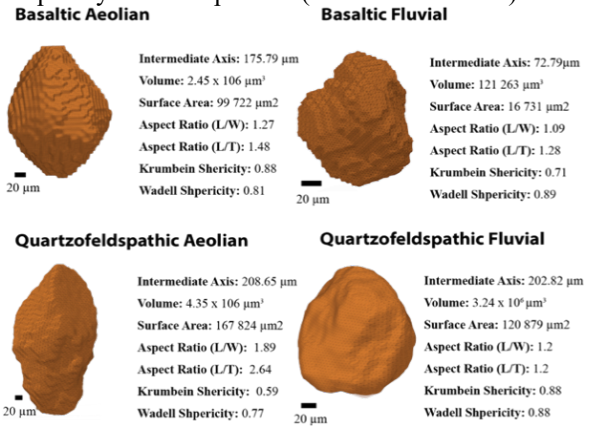

Fig. 1: Virtual particles created from µXCT scans. For each particle various 2D and 3D parameters can be calculated.

Many methods and instruments exist to analyze particle shape and size. Particle size analysis is traditionally done through sieving [3]. Laser diffraction technology has improved the speed and numbers of particle size counts as compared to sieving but lacks shape analysis [4]. Dynamic image analysis (DIA) is a state-of-the-art method in which the projected area of a particle is used to calculate 2D size and shape parameters (e.g., circularity) [5]. µXCT for 3D particle analysis is a less explored technique in sedimentology and geomorphology applications. It has the potential to reveal new insights into particles shapes and their relationships with process and mineralogy.

Method: Aeolian and fluvial basaltic and quartzofeldspathic samples were collected from environments in Iceland and Texas. Samples from Iceland were collected as part of the Semi-Autonomous Navigation for Detrital Environments project. This project examines physical and geochemical changes to sediments along basaltic sediment transport pathways with robotic science operations. Samples consists of (i.) quartzofeldspathic sediment from a wind-blown dune in Padre Island, TX and (ii.) quartzofeldspathic sediment from a lateral bar on Brazos River, TX, (iii.) basaltic sediment from a wind-blown vegetated dune in Iceland and, (iv.) basaltic sediment from a lateral bar on a river in Iceland.

Samples were split and sieved to a range of 63 to 500 µm. The split sample was then mixed with epoxy in a small tube of diameter ~3mm with length 12 mm. This allows the particles to be suspended when scanned allowing individual particles to be segmented during processing. The samples were scanned at a resolution of 6.07 µm/voxel at the Astromaterials X-ray Computed Tomography Lab at NASA JSC. The data produced are 2D TIFF images which when stacked creates a 3D image. The Garboczi/ Bullard method was used to segment and analyze the data [6]. It provides mathematical information that can be used to re-generate the particle as desired in any kind of 3D model, at any location and orientation, or to generate virtual particles that are forced to have the same statistics. It uses the burning algorithm to identify particles and then spherical harmonics series fitting and voxel counting to generate and store particle size and shape, 3D images of the particles, and geometrical information for each particle [6].

This approach is specifically for star-shaped particles. A particle is star-shaped if there is a fixed point, *O*, in its interior for which a straight line drawn from that point to any other point inside the object lies entirely within the object [7]. The nonstar-shaped particles are separated and not included in the data presented in this abstract.

Results: Fig. 1 shows four virtual particles, one from each of the samples. Intermediate axis length, surface area, volume, aspect ratio, and sphericity are calculated for each particle.

Because we generated 3D virtual particles, any size and shape parameter can be calculated. One of the more well-known parameters is grain size. This is based on the intermediate axis of the particle. Fig. 2 shows the distribution of the grain size of particles in each

environment through the use of a histogram and a boxplot to summarize the data. The basaltic aeolian and basaltic fluvial samples have modes of 125 µm and 100 µm respectively. The mean grain size for the basaltic aeolian and fluvial particles are 134 and 107 µm respectively. The quartzofeldspathic aeolian sample mode is 250 µm with a mean grain size of 239 µm. The quartzofeldspathic fluvial appears bimodal with modes of 63 and 175 µm, with a mean grain size of 152 µm.

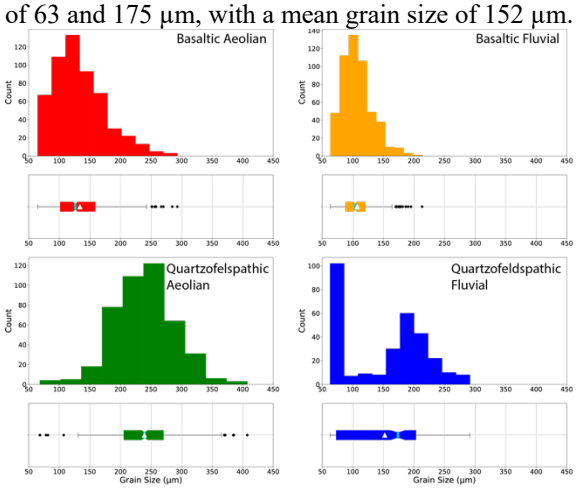

Fig. 2: Histogram, cumulative distribution plot and boxplot showing grainsize of particles in four samples: (i)Basaltic Aeolian, (ii) Basaltic Fluvial, (iii) Quartzofeldspathic Aeolian and (iv) Quartzofeldspathic Fluvial. Median is represented as a cyan line and mean is a white triangle.

Sphericity is calculated using volume and surface area, which makes it a true 3D parameter. We calculate sphericity as the ratio of the surface area of a sphere with the same volume as the particle to the actual surface area of the particle [8]. A sphericity of 1 represents a sphere.

Fig. 3 shows sphericity plotted with grain size. All particles have a sphericity above 0.5. Greater sphericity occurs with larger grain size for all samples except quartzofeldspathic aeolian, which shows no correlation. The quartzofeldspathic aeolian sample, however has the highest sphericity compared to all the other samples. The aeolian samples are more spherical than the fluvial samples.

Discussion: Results show similar values in grain size and sphericity for the fluvial and aeolian basaltic samples, which may indicate the aeolian samples are reworked fluvial sands or vice versa. The aeolian quartzofeldspathic samples show greater sphericity than the fluvial. The greater sphericity in the aeolian samples is likely due to the high energy of saltation, which dominates this mode of transport [9]. The positive trend in sphericity and grain size is consistent with the tendency of smaller grains to resist rounding through abrasion[10]. The quartzofeldspathic aeolian sample is the best sorted, which may explain the lack of fines with lower sphericity.

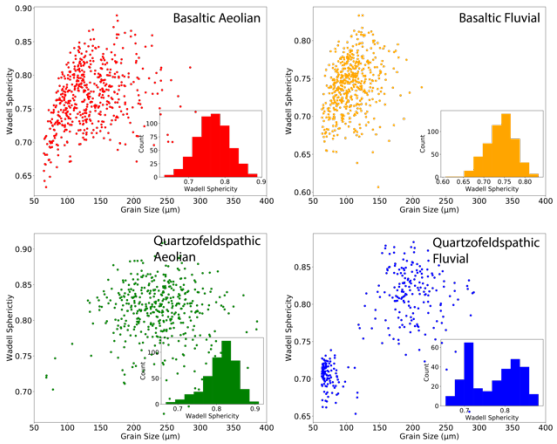

Fig. 3: Scatter plot showing sphericity vs grain size and histogram of sphericity of particles in four samples: (i)Basaltic Aeolian, (ii) Basaltic Fluvial, (iii) Quartzofeldspathic Aeolian and (iv) Quartzofeldspathic Fluvial.

The mode of 63µm for the quartzofeldspathic fluvial is abnormally high and may be an indication of error in the process. The data require further analysis by (i)comparing µXCT results to DIA results, (ii)looking at the raw data including the virtual particles for the nonstar-shaped particles, and (iii)by taking a closer look at the TIFF images to determine how much noise is being generated in the data.

Conclusion: This study examines the value of 3D analysis for sedimentology and geomorphology of Earth and other planetary bodies, as well as for potential engineering applications. µXCT is an emerging in-space technology that could prove important for development of lunar and Martian resources for science and engineering applications. It is especially useful when samples are limited and has the advantage of being a nondestructive method.

References: [1] Tucker, M. E. (2003). *Sedimentary rocks in the field*. [2] Krumbein, W. C. (1941). *Journal of Sedimentary Research*, *11*(2), 64-72. [3] Day, Paul R. (1965) *Methods of Soil Analysis: Part 1,* 9: 545-567. [4] Eshel, G. et al. (2004). *Soil Science Society of America Journal*, *68*(3), 736-743. [5] Tysmans, D. et al. (2006). *Particle & Particle Systems Characterization*, *23*(5), 381-387. [6] Garboczi, et. Al (2020). *J. Vis. Exp. (166),* 249: 241-252. [7] Bullard, J. W., & Garboczi, E. J. (2013). *Powder technology*, *249*, 241-252.[8] Wadell, H. (1932). *Journal of Geology:* 40(5), 443-551. [9] Miller, K. L., Reitz, M. D., & Jerolmack, D. J.(2014). Geophysical Research Letters, 41(20), 7191-7199. [10] Ziegler, V. (1911) The Journal of Geology, 19.7: 645-654.